Microelectronic Engineering 104 (2013) 75–84

Contents lists available at SciVerse ScienceDirect

Microelectronic Engineering

journal homepage: www.elsevier.com/locate/mee

Packaging-compatible wafer level capping of MEMS devices

Rajarshi Saha, Nathan Fritz, Sue Ann Bidstrup-Allen, Paul A. Kohl *

School of Chemical and Biomolecular Engineering, Georgia Institute of Technology, Atlanta, GA 303320-0100, United States

ARTICLE INFO

Article history:
Received 31 October 2011
Received in revised form 24 September 2012
Accepted 6 November 2012
Available online 3 December 2012

Keywords:
MEMS
Packaging
Air-cavity

ABSTRACT

A cost-effective, wafer-level package process for microelectromechanical devices (MEMS) is presented. The movable part of MEMS device is encapsulated and protected while in wafer form so that commodity, lead-frame packaging can be used. A polymer epoxycyclohexyl polyhedral oligomericsilsesquioxanes has been used as a mask material to pattern the sacrificial polymer as well as overcoat the air-cavity. The resulting air-cavities are clean, debris-free, and robust. The cavities have substantial strength to withstand molding pressures during lead-frame packaging of the MEMS devices. A wide range of cavities from 20 μm × 400 μm to 300 μm × 400 μm have been fabricated and shown to be mechanically stable. These could potentially house MEMS devices over a wide range of sizes. The strength of the cavities has been investigated using nano-indentation and modeled using analytical and finite element techniques. Capacitive resonators packaged using this protocol have shown clean sensing electrodes and good functionality.

1. Introduction

In the past decades, many advances have been made in the fabrication of MEMS structures. However, proper packaging presents a pivotal challenge to their overall potential [1]. For typical MEMS based products, packaging expense can be as high as 20–40% of the products total material and assembly cost [2]. While certain MEMS devices require special conditions for operation, a cost efficient, IC compatible packaging process would significantly improve the cost and application for a variety of MEMS devices.

There are various wafer-level packaging methods available commercially. Wafer level packaging methods include interfacial bonding of a Pyrex glass lid, which has a similar coefficient of thermal expansion to silicon [3]. The lid is anodically bonded to the MEMS wafer at approximately 400 °C by applying a negative voltage to the glass. Other interfacial bonding methods include plasma-activated bonding. Electrical feed-throughs are made through a via in the lid wafer. Bonding with intermediate melting materials, such as low melting temperature glass and solder have also been used [3]. These bonding techniques can be applied to a non-planar surface and hence lateral electrical feed-through, which causes a non-planar surface, can be used. MEMS devices can also be encapsulated using surface micromachining [3]. The cavity can be made by etching a sacrificial layer and the openings needed for removal of the temporary placeholder material are plugged by deposition of a sealing material. A vacuum cavity is required for some MEMS devices, such as resonators and infrared sensors. Electrical feed-through structures for the electrical interconnection are indispensable for wafer level packaging [3].

Air–gap structures have been used in micro and nanosurface micromachining processes for fabricating MEMS and nanoelectromechanical systems (NEMS) capable of in-plane and through-plane motion [4]. These cavity structures use a low temperature, thermally decomposable sacrificial material, especially desirable for isolating electrical and mechanical parts. The overcoat material on these structures should be tolerant of stress and temperature effects and offer a convenient diffusion path for the decomposition by-products. Furthermore, a metal overcoat is often necessary for hermetic sealing and increased mechanical strength of the air-cavity [5]. Overall, the materials for sacrificial layer, overcoat and hermetic seal should be compatible with existing processes and offer good layer-to-layer adhesion.

Numerous reports of wafer level packaging of MEMS structures using air-cavity technology have been published. Joseph et al. used the decomposition of Unity^R 2303 polymer through a thin SiO_2 film to fabricate an air-cavity and package MEMS resonators [6]. The processing protocol is complex because an oxide mask is first used to pattern the Unity layer. An oxide/polymer (Avatrel) overcoat was used for mechanical strength and to expose the bond-pads. Similar methods were used to package varactors and accelerometers. An improvement in the performance of the MEMS devices was observed after packaging with this air-cavity approach [7]. Monajemi et al. successfully packaged a wide range of MEMS devices using both photodefinable and non-photodefinable Unity to form the air-cavity. However, photodefinable Unity was found to

* Corresponding author.
E-mail address: kohl@gatech.edu (P.A. Kohl).

0167-9317/$ - see front matter © 2012 Elsevier B.V. All rights reserved.
http://dx.doi.org/10.1016/j.mee.2012.11.010

leave a residue from the photo-active compound after decomposition which could affect the performance of the device [8]. Rai-zadeh et al. packaged a tunable inductor using Unity and Avatrel (overcoat), however, a separate material was used to pattern the sacrificial polymer [9]. Reed et al. developed a compliant wafer-level process containing air-cavities that offer high on-chip current and enable terabit/s bandwidth [10].

In this study, air-cavities were fabricated with a unique polymeric material, epoxycyclohexyl polyhedral oligomeric silsesquioxanes (POSS), that enables patterning the sacrificial material, polypropylene carbonate (PPC), as well as providing structural rigidity as an overcoat. POSS is a hybrid organic/inorganic dielectric which has interesting mechanical and chemical stability for use as a permanent dielectric in microfabrication of electronic devices [1,4,14]. POSS was used to pattern the PPC and used as the air-cavity overcoat material. Hence, this will cut down on the number of processing steps and consequently the cost of packaging as well. We also report a novel tri-material system consisting of PPC/POSS/metal to create air-cavities which could house a wide range of MEMS devices on a wafer level irrespective of device size and functionality.

The air-cavity system described here also has the flexibility to vary the strength of the superstructure surrounding the air-cavity according to the lead-frame packaging requirements. Lead frame package is accomplished by using epoxy molding at high pressure. Schematic drawings of compression and injection molding of air-cavity packages are shown in Fig. 1. The injection molding process forces the epoxy molding compound (EMC) around the device in the mold. This is the more traditional process for chip packaging and uses high molding pressures (e.g. 10 MPa). The compression molding process molds only the top side of the device and uses lower pressure than injection molding (e.g. 4–10 MPa). Compression molding is commonly used in chip-stacking packages. The lead frame package process can be metallized after cavity formation to form hermetic cavities or a high degree of mechanical support. A second novel packaging approach demonstrated in this study is the in situ decomposition of the sacrificial material during the epoxy molding process. This is especially useful for large, semi-hermetic lead frame packages. The new, chip-level package retains the sacrificial during the molding process and performs the decomposition step (cavity formation) during the epoxy cure step once the epoxy overmolding material is rigid, preventing cavity collapse. The in situ method allows molding and release of very large channels and cavities for a range of packaged devices where hermetic sealing is not necessary.

2. Materials and experimental methods

PPC was used as the sacrificial material, as described previously [1]. It is a copolymer of carbon dioxide and propylene oxide, polymerized at high pressure in the presence of catalyst [11]. High-purity forms of the PPC exist in regular, alternating units without ether-linkage impurities in the backbone. PPC decomposes by chain scission and unzipping mechanisms. Decomposition proceeds via chain unzipping at low temperatures because the cyclic monomer is thermodynamically favored over the straight-chain polymer [12]. At higher temperature, chain scission competes with the unzipping decomposition mechanism. PPC is an attractive sacrificial material for microelectronics because it decomposes cleanly into low-molecular-weight products with little residue in inert and oxygen-rich atmospheres [13]. Air cavities were formed by decomposing the PPC layers and allowing the products diffuse through the overcoat, thus leaving a gaseous void [1]. Several other polycarbonate systems were investigated for lower or higher decomposition properties. Additives, such as a photo acid generator (PAG), can be added to PPC to lower decomposition temperature. Fig. 2 shows a dynamic thermal gravimetric analysis (TGA) of pure PPC and a 3 wt.% PAG loaded PPC. The PAG material thermally decomposes into an acid decreasing the decomposition temperature of the PPC. When exposed to ultraviolet radiation, the acid is generated at a lower temperature catalyzing the PPC decomposition at temperatures as low as 100 °C. Since, epoxy curing after injection molding takes place at ~180 °C, we wanted to investigate another sacrificial material that decomposes preferably at the same temperature which would allow cavity-creation and epoxy curing simultaneously. Hence, polyethylene carbonate (PEC) was investigated as a relatively high temperature sacrificial material. PEC has similar physical properties to PPC and decomposes at 180 °C.

The properties of the overcoat material are important in the design of the air-cavity structure. The use of a spin-coated, photosensitive, hybrid inorganic/organic dielectric has been previously shown to be an effective overcoat material [1,4,14]. In this work, a photodefinable dielectric form of POSS was created by the addition of a photo-initiated catalyst to POSS. POSS was dissolved in mesitylene making a 40 wt.% or 60 wt.% solution. An iodonium photo-acid generator was added at 1 wt.% of POSS and sensitizer at 0.33 wt.% of POSS so as to make the formulation photosensitive at 365 nm.

Deep trenches in 100 mm diameter (100) silicon wafers were etched using the Bosch process. These trenches resemble actual capacitive and piezoelectric MEMS devices that were fabricated.

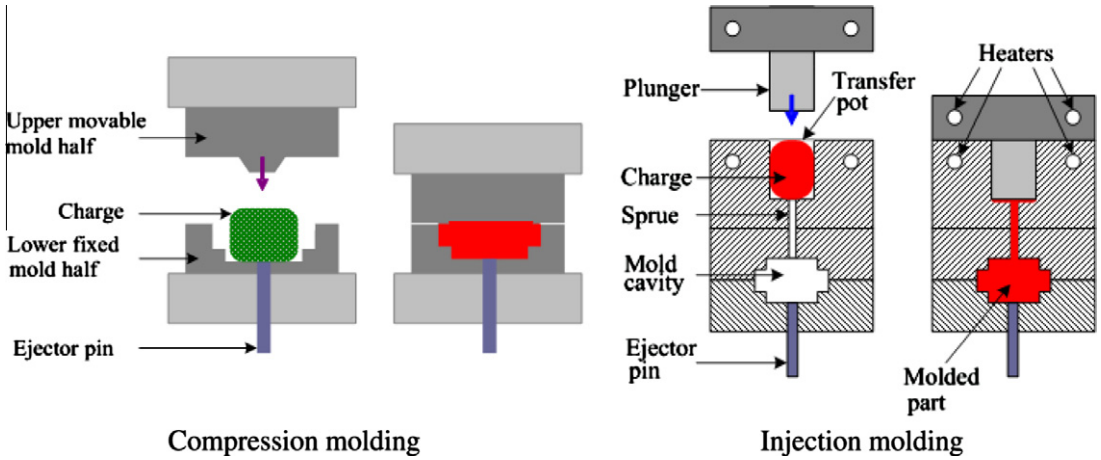

Fig. 1. Schematics of compression and injection molding processes.

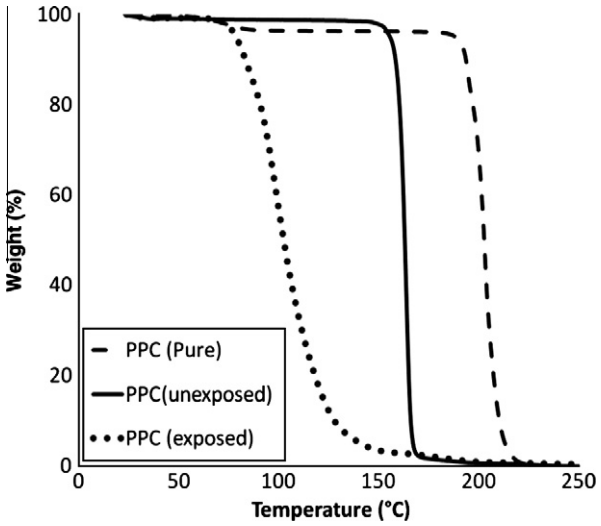

Fig. 2. Dynamic TGA at 5 °C/min showing the effect of a 3 wt.% PAG loading on PPC.

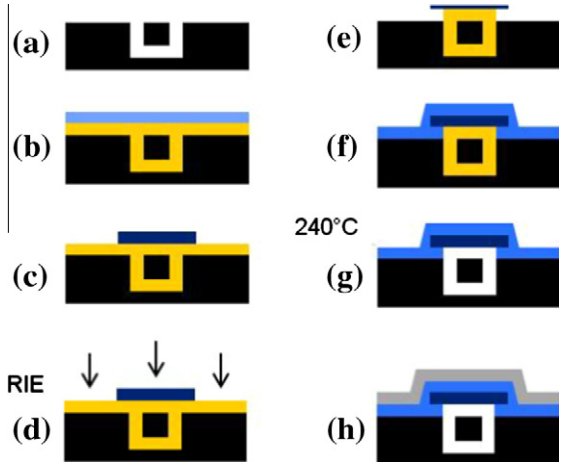

Fig. 3. Process flow for Wafer level package. (a) Wafer with simulated devices, (b) spin coat of PPC and then POSS, (c) pattern POSS, (d) dry etch (RIE) PPC, (e) thin layer (remaining) of POSS after PPC etch from field regions, (f) spin coat POSS overcoat and pattern, (g) decompose PPC, (h) evaporate metal overcoat for hermetic seal.

Trench widths varied between 2 and 6 μm and the trench-depth was approximately 6 μm. Each device had in between 2–6 trenches depending on the type of device and each wafer had several hundred devices. Wafer-level packaging was then carried out using the PPC/POSS material system. After completing the packaging steps, the wafers were diced with a diamond saw and characterized using scanning electron microscopy (SEM), nano-indentation, and tape test for metal adhesion. A complete process flow is shown in Fig. 3. PPC was initially spin-coated on the silicon trenches and softbaked on a hot-plate at 100 °C for 5 min. Several spin-coating steps were required for deeper and wider trenches. The PPC thickness varied between 3 and 4 μm after baking. For patterning the PPC, POSS was spin-coated at 4000 rpm resulting in a 0.6 μm thick film (Fig. 3(b)). POSS was pre-baked at 85 °C for 5 min, patterned at 365 nm and post-baked at 85 °C for 5 min. POSS was spray developed using isopropyl alcohol (Fig. 3(c)) [14]. PPC was reactive ion etched using a 6% CHF_3 and 94% O_2 plasma that resulted in a PPC/POSS etch rate selectivity of 24 (Fig. 3(d)). The PPC etch rate was 0.66 μm/min. The overcoat POSS was then spin coated to a thickness of 3–6 μm and patterned (Fig. 3(f)). It was baked according to the first POSS layer. Finally, the PPC was decomposed at 240 °C for 4–10 h in a N_2 environment using a step-wise ramp-rate described elsewhere [15]. The wafers were subjected to a short duration oxygen plasma prior to metallization to improve metal-to-POSS adhesion. Aluminum was evaporated to a thickness of 0.7–2 μm and patterned to expose the electrode areas (Fig. 3(g)). For more rigid overcoats, Cu (1–3 μm) was used instead of aluminum. Ti (50 nm) was the adhesion promoter for the copper metal overcoat. Different cavity-types with dimensions and overcoat thickness are tabulated in Table 1.

Table 1
A list of cavity-sizes and metal overcoats used in this work.

Simulated devices	Width (μm)	Length (μm)	Metal overcoat (μm)
Capacitive (small) resonator	10–50	300–400	Al: 0.7 μm, Cu: 1.5 μm, 3 μm
Capacitive (large) resonator	50–150	300–400	Al: 0.7 μm, 2 μm, Cu: 1.5 μm, 3 μm
Piezoelectric resonator	150–200	300–400	Cu: 1.5 μm

After fabrication, the individual packages were inspected for thermo-mechanical cracking at the edges using an Hitachi FE3500 SEM. Close inspection of the trenches was done using a focused ion beam (FIB) (FEI Nova Nanolab) sectioning tool. The wafer was diced and the shape and cleanliness of the cross-section examined. The small and large devices were diced and inspected. Nano-indentation was carried out to assess the mechanical strength of the cavities. A pressure test was developed using a Hysitron nano-indenter. The nano-indenter used a 20 μm diameter conospherical tip. The test location at the center of 30–50 μm wide cavities did not encounter resistance from the side-walls during experimentation. The cavities were indented at room temperature to a force of 8.5 mN. A cross-hatch tape test was used to determine the adhesion strength of thicker metal overcoats [16]. After the tape has been applied and pulled off, the cut area was then inspected and rated.

Transfer molding consisted of injecting the epoxy molding around the device into the desired shape. Transfer molding was carried out at 175 °C for 105 s at 10 MPa and then post mold cured at 175 °C for 8 h, unless otherwise noted. Compression molding was completed on several packages as well. Compression molding places the molding compound on the device and applies a relatively low pressure (e.g. 4 MPa) to form the packaged shape. Samples were cross-sectioned to evaluate the extent of damage. Raman spectroscopy was carried out to investigate debris left in the cavity. Focused ion beam images confirmed debris-free cavities prior to molding. Furthermore, to prevent collapse during molding due to the high pressure, large cavities were metallized with a thicker copper coat. Titanium was used as the adhesion layer. Subsequent packages were molded and observed for cavity damage.

Two dimensional mechanical analysis of air-cavity packages was carried out using Ansys (ANSYS 13.0) finite element modeling. A linear, elastic isotropic model assumed perfect adhesion between polymer and metal layers. A rough, frictional contact (with no slip; infinite coefficient of friction) between overcoat and wafer under high pressure was assumed as a boundary condition. Modeling of all layers was done with PLANE42 elements: a 2D structure with four nodes. Contact between POSS and the wafer was modeled using CONTAC171 and TARGE169 elements compatible with PLANE42. Both are line elements. The molding pressure was applied from the top and the cavity deflection was measured and compared to experimental conditions. A comparison was also made with a standard analytical solution. The effect of different metals and thicknesses on the deformation and stress distribution

within the cavity was studied. Conclusions drawn from simulations helped in the design of stronger overcoats for larger cavities.

The packaging protocol thus developed has been successfully verified on an actual capacitive resonator approximately 100×400 μm in size. The electrical performance of the device was evaluated after packaging.

3. Results and discussion

3.1. Narrow features (<100μm)

The first samples studied were smaller devices packaged using 40% POSS as the masking material for patterning the PPC sacrificial material and the cavity overcoat material. The cavity width was varied between 20 and 50 μm and the length varied between 200 and 600 μm. To prevent cavity cracking or rupture, the PPC decomposition process was modified from a constant thermal ramp rate to a constant weight percent decomposition rate [15]. The constant rate of decomposition allows for the more orderly diffusion of decomposition products through the overcoat avoiding high internal pressures. Thermogravimetric analysis of the polymer was used to determine the parameters for the constant rate of decomposition [15]. The reaction kinetics can be expressed as the nth order Arrhenius relationship, as shown in Eq. (1).

$$r = Ae^{\frac{-E_a}{RT}}(1 - rt)^n \tag{1}$$

where r is the decomposition rate, A is pre-exponential factor, E_a is the activation energy (kJ/mol), T is the temperature (K), and t is time (s). The decomposition reaction was determined to be first order ($n = 1$) with a pre-exponential factor (A) and activation energy (E_a) of 9×10^{12} min^{-1} and 120 kJ/mol, respectively. Eq. (1) can be rearranged for temperature (T) vs. decomposition time (t) as shown in Eq. (2). A rate of 0.25 wt.%/min for the decomposition was used to decompose the PPC. No degradation of the cavities was observed.

$$T = \frac{E_a}{R}\left[ln\frac{A(1 - rt)^n}{r}\right]^{-1} \tag{2}$$

The SEM cross-sections are shown in Fig. 4(a) and (b) and exhibit debris-free cavities with robust, sturdy overcoats. The overcoat stability allowed the cavity to retain the shape of the original PPC structure under the overcoat. Close inspection of the trenches using FIB, Fig. 4(b), also showed clean cavities. Apart from the inadvertent deposition of material from the FIB, the trenches were debris-free. PPC can form non-uniform shapes during spin-coating which leads to occasional dips within the overcoat just above the trench. Such dips do not affect the functionality of our MEMS devices as long as the overcoat does not come in contact with the device area. However, since the cavity height is reduced above the trench, these areas remain vulnerable during contact or injection molding. Also, these dips become larger if the trench width is increased. Adjusting the PPC thickness by changing the polymer viscosity and spin-coat conditions can mitigate non-planar problems. Spin-coating multiple layers followed by drying (i.e. soft baking) at room temperature can improve the amount of reflow into the trench. The room temperature soft bake prevents thermal reflow of the PPC into the trench and the multiple layers improve planarization of the device features.

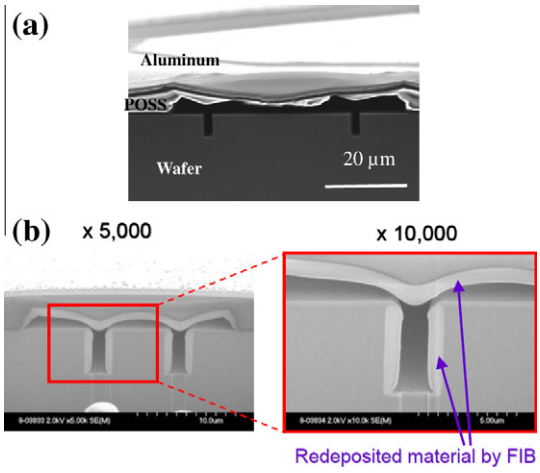

Fig. 4. Air-cavities formed on smaller simulated devices show debris-free decomposition.

3.2. Wider features (>100μm)

The overcoat formulation was adjusted for different cavity dimensions to provide better uniformity. For large cavities (>100 μm wide), thin overcoat layers tend to crack during PPC decomposition and the overcoat is unable to provide the mechanical strength necessary to support the cavity, as shown in Fig. 5(a). Changing the POSS-to-solvent ratio helps tune the properties of the overcoat. The polymer concentration could be raised from 40% to 60% for better control of overcoat uniformity and thickness. The 60% POSS formulation results in a lower degree of film cracking (compared to 40% formulation) during thermal decomposition. The thicker film improves coverage and planarization on the edges of the cavity, as shown in Fig. 5(b). Alternatively, several spin coatings of the 40% POSS formulation produced a crack-free cavity with similar edge coverage to the 60% POSS while maintaining an overall thinner film as shown in Fig. 5(c). In Fig. 5(c), the cavity was snapped mid-way and hence shows a wavy surface topography. The decomposition ramp rate was lowered when thicker overcoats were used so as to lower the pressure build-up. As shown in Fig. 6(a), a 4 h decomposition recipe is not long enough to fully decompose the PPC. Higher decomposition temperatures lead to cracking of the overcoat due to pressure build-up during decomposition, as shown in Fig. 6(b). A slow ramp-rate followed by a long temperature hold is necessary to form near-perfect air-cavities with sharp side-walls. In our experiments, 0.5 °C/min ramp-rate and 6–8 h hold at 240 °C was necessary for cavities with widths from 50 to 150 μm, Fig. 6(c). The protocol for packaging capacitive resonators (~50–150 × 400 μm) had to be modified slightly to carry out wafer-level packaging of devices larger than 150–300 × 400 μm.

Besides being quite large (~200 μm wide and 500–600 μm long), these devices had complex topography. By using a thicker overcoat (60% polymer) and multiple spin-coats we were able to successfully package such complex geometries after a 10 h decomposition regime for the sacrificial polymer. The resulting cavities (Fig. 7) were found to be clean and mechanically stable. Hence, for smaller devices (less than 150 μm wide), multiple spin coats of 40% polymer with 6–8 h decomposition times were adequate. However, devices with widths larger than 150 μm require multiple spin-coatings of 60% polymer mixtures with longer decomposition times. The decomposition time depends on the thickness of PPC. Wider cavities require thicker PPC films to prevent cavity collapse during decomposition or molding.

3.3. Mechanical strength and molding of cavities (<100 μm)

The robustness of the cavity overcoats was evaluated using nanoindentation. For a 3 μm POSS overcoat (40% POSS formulation) and 0.7 μm thick aluminum metallization, complete collapse for a 3.5 μm tall cavity was observed at 4 mN as shown in Fig. 8(a).

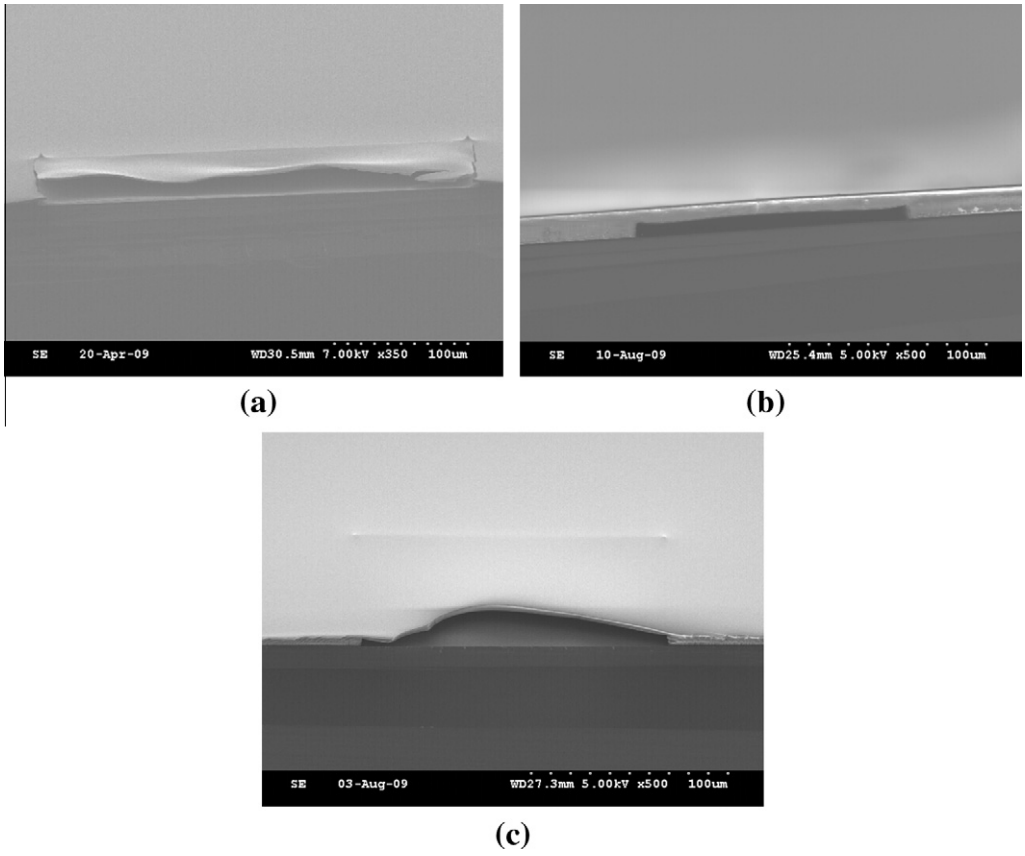

Fig. 5. Cracked overcoat after decomposition for large cavities. (a) To prevent overcoat thermomechanical failure, (b) a thicker overcoat (40% solvent) or (c) multiple (X5) spin-coats of conventional (60% solvent) could be used.

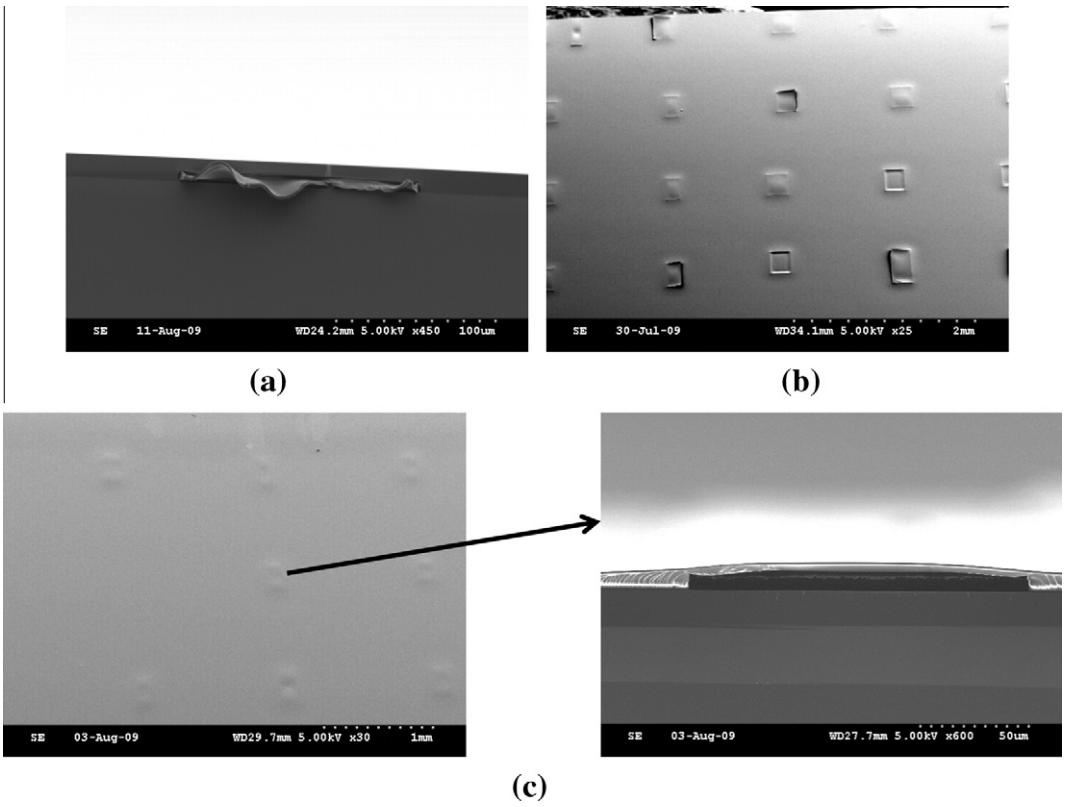

Fig. 6. Decomposition of PPC to form air-cavities. (a) Incomplete decomposition through thick overcoat reveals presence of PPC. (b) Higher decomposition temperature causes overcoat cracking due to pressure build-up. (c) Optimized time and temperature leads to mechanically robust, stable and clean cavities.

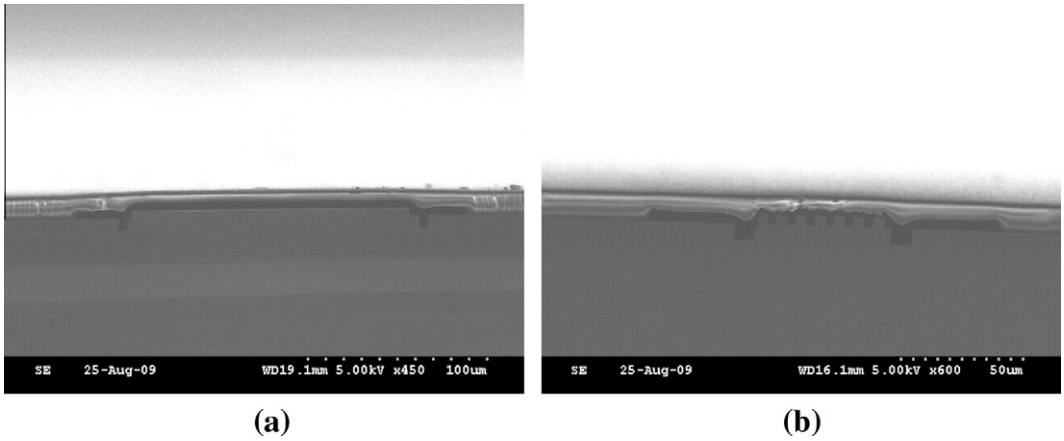

Fig. 7. Large air-cavities to package piezoelectric devices. These simulated devices have wider trench-widths and uneven topography. The overcoat after decomposition remains stable and the air-cavities are clean.

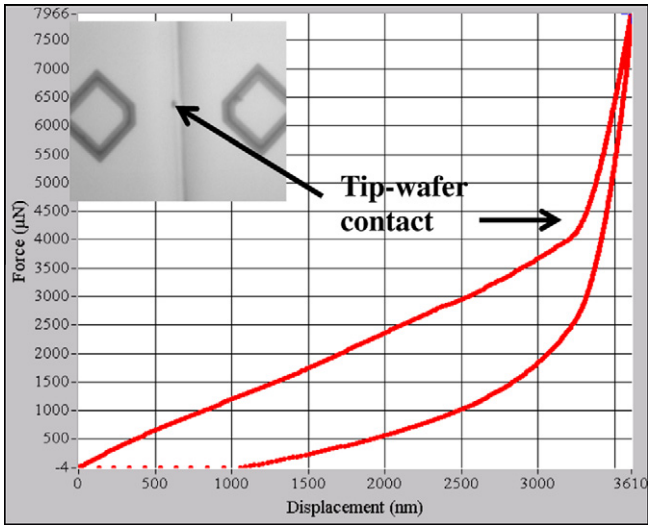

Fig. 8. Nanoindentation of cavities show complete collapse at 4 mN for a 20 μm wide cavity with a 1 μm aluminum overcoat (inlay shows nanoindentation spot on the cavity). The deflection of the overcoat decreases as the Al thickness increases or if its replaced by copper (Table 2).

Table 2
Cavity deflection under nano-indentation with different metal overcoats (E: elastic modulus, t: thickness, F_{max}: force, d_{max}: deflection). Cavity strength (low deflection) can be improved by using thicker metal overcoats. (40% solvent) could be used. (cavity size ~10–40 μm).

Metal	E (GPa)	t (μm)	F_{max} (mN)	d_{max} (μm)
Al	70	0.7	4	3.5
Al	70	2	8.5	1.1
Cu	128	1.5	8.5	1.3

This translates to a cavity-strength of 51 MPa. Cavities with widths from 10 to 40 μm were tested. The tip was placed in the middle of the cavity to minimize side-wall effects. The nano-indentation results have been tabulated in Table 2. If the aluminum is replaced by 1.5 μm thick copper; the rigidity increases due to the higher elastic modulus of copper compared to aluminum. As shown in Table 2, the cavity deflects 1.3 μm at 8.46 mN. The deflection is similar to a 2 μm aluminum overcoat. This shows that for an air cavity design with a large deflection, air cavity collapse can be prevented by increasing the modulus of the overcoat material and/or increasing overcoat thickness.

Once the wafer level package cavities are created they can then be diced and molded for lead frame packaging. Cavities were molded using an epoxy molding compound (EME-G700E). It was observed that the initial cavities with 0.7 μm aluminum overcoat and 20 μm width, were able to withstand a molding pressure of 4 MPa, Fig. 9(a). However, they collapsed completely at 10 MPa pressure, Fig. 9(b). The debris inside the cavity in Fig 9(b), was studied using Raman spectroscopy and the spectra shown to be polishing material. Larger cavities (75 μm wide) were observed to completely collapse at both pressures. If we replace the aluminum overcoat with a 3 μm thick copper overcoat, the cavities were able to withstand higher pressure. It was observed that cavities as wide as 100 μm were able to withstand 10 MPa pressure and deform only slightly, Fig. 9(c). In order to increase the cavity strength, for a specific cavity-width, one needs to increase the metal thickness or elastic modulus. Increasing the cavity height would also be an advantage because a larger deformation would be necessary for device failure. However, this would require thicker PPC coatings and subsequently thicker POSS overcoats for conformal coverage. The cavity deflections at a certain molding pressure closely match the FEM and analytical models as explained later. Increasing the POSS overcoat thickness will affect the cavity strength; however the elastic modulus of POSS is approximately 4 GPa which is much lower than either aluminum or copper. Thicker metal layers can also be problematic due to residual stresses.

The 2D FEM model was used to understand the pressure limits in cavity deflection during molding. The normalized Von Mises stress was calculated for specific configurations. As seen from Fig. 10, the FEM model shows the deflection of a 40 μm wide cavity with 0.7 μm thick aluminum at 4 and 10 MPa pressure. At 4 MPa pressure, the measured deflection is 1.5–2 μm which is essentially the same as the simulated value of 1.5 μm. At 10 MPa atm pressure, the experimental cavity completely collapsed to the surface showing no presence of a cavity. However, the 10 MPa simulation shows collapse in the center of the cavity. The simulation included only elastic properties. The full collapse may involve the plastic deformation of the overcoat.

The FEM results were compared to a previously derived analytical model, the rectangular bulge equation, to correlate the deflection values obtained from the finite element technique, as shown in Eq. (3). [17]

$$P = \frac{2ht\sigma_0}{a^2} + \frac{4h^3Et}{3a^4(1-\nu^2)} \tag{3}$$

where, P is the molding pressure. The overcoat material properties are accounted for with E being the elastic modulus, υ is the poisson

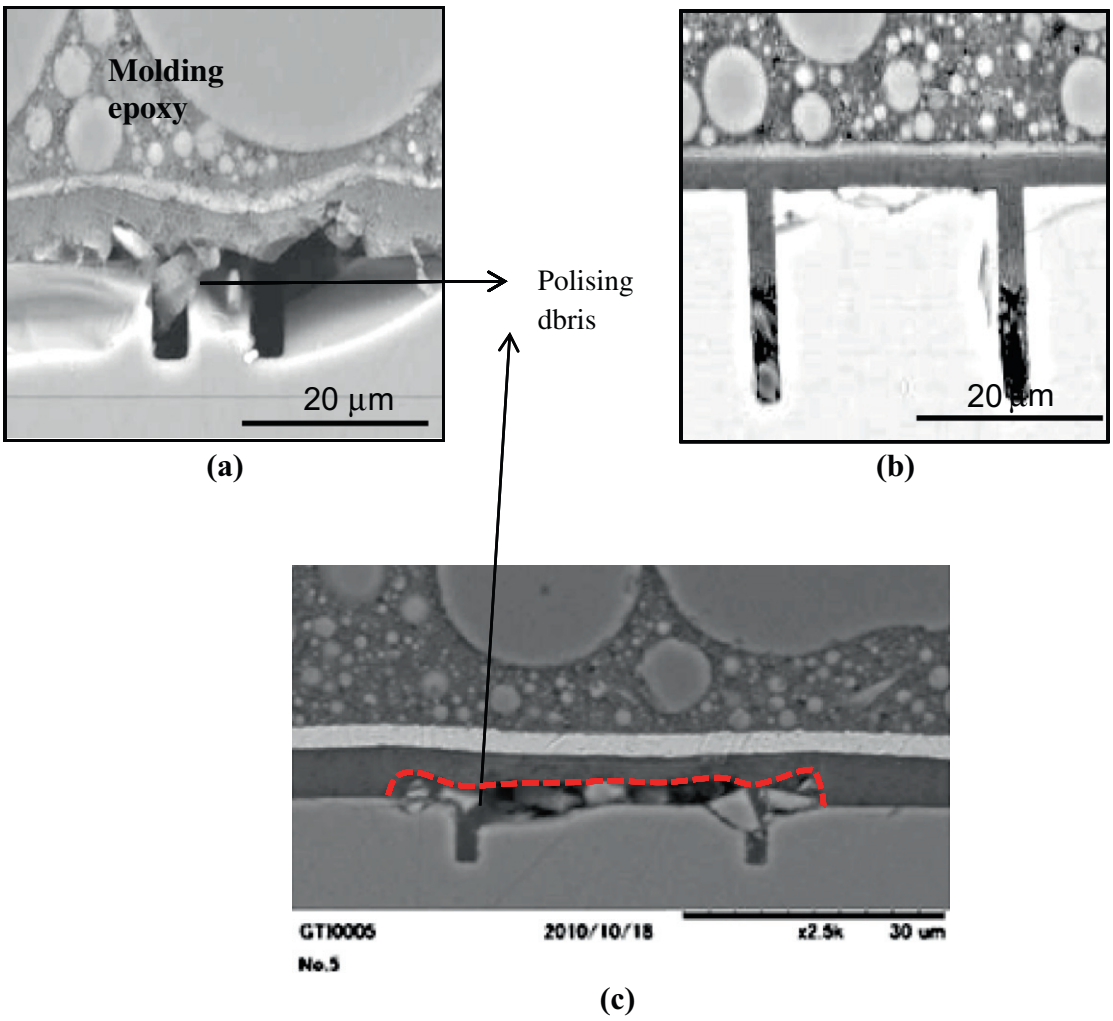

Fig. 9. (a) A 20 μm wide with 1 μm Al overcoat cavity stays intact under 4 MPa compression molding. (b) A 50 μm wide cavity completely collapses under 10 MPa compression molding but (c) sustains the same pressure with a 3 μm copper overcoat undergoing 0.5 μm deflection.

ratio, and σ_0 is the initial film stress. The variables a, t and h refer to the geometry of cavity. The value a is the half of the width of the cavity, t is the thickness of the overcoat, and h the height of the maximum deflection of the overcoat from its initial location.

The elastic modulus of the overcoat was assumed to be dominated by the metal portion of the metal-polymer composite because the modulus of the metal is about 30 times greater than that of the polymer. The initial film stress, σ_0, of the annealed, electrodeposited copper film was found to be approximately 30–100 MPa depending on thickness from the literature [20]. When the initial calculations were made the first term of the equation was significantly smaller than the second term using literature values. The first term was assumed to be negligible for further calculations in estimating the deflection of the cavity. The two controllable factors for design is the metal thickness and adjustment of the cavity height to prevent total deflection.

As shown in Fig 10, the corresponding deflection values were 2 μm and 2.8 μm for 40 and 10 MPa pressure, respectively. These values match both experimental and FEM values. The overall stress in the overcoat and deflection of the air-cavity could be further reduced through optimization of the thicknesses and annealing conditions. For example, a 10% decrease in the maximum stress along the cavity sidewalls was observed by forming a 30° slope in the side-walls. Changing the cavity from a straight side-walled structure to a sloped sidewall through the patterning and reflow of the PPC will help optimize a cavity that is more resistant to stress as has been published earlier [15]. The total deflection of a 3 μm copper overcoat at 10 MPa pressure was found to be 0.56 μm from Eq. (3), which is the same as the experimental deflection in Fig. 9(c).

Process modifications: The adhesion between POSS and the substrate and POSS the metal overcoat was found to be excellent. However, in order to increase the cavity strength, a thicker metal overcoat was required. When thicker metal overcoats were used, e.g. 2 μm aluminum, the residual stress during e-beam deposition was great enough to cause adhesive failure between the aluminum and the POSS. An oxygen plasma clean was used prior to metal deposition to improve the adhesion. For thicker copper overcoats, copper was electroplated at low current density on the sputtered seed layer followed by annealing at 180 °C for 1 h to reduce the internal stress. After annealing, the metal film exhibited excellent adhesion.

3.4. Simultaneous molding and PPC decomposition

The results presented above show that there are numerous methods to strengthen the overcoat and fabricate ever wider cavities. However, there is a limit to the metal thickness (e.g. metal adhesion and residual stress) and optimization of the cavity shape

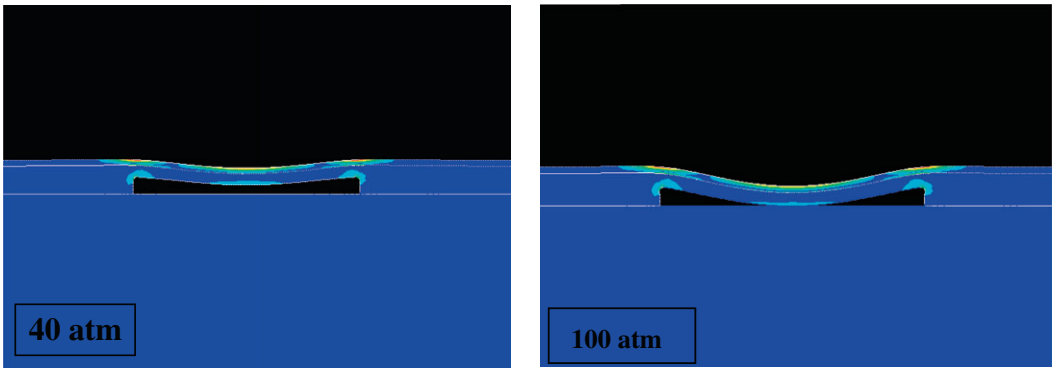

Rectangular "Bulge" equation:

$$P = \frac{4}{3}\frac{h^3}{a^4}\frac{Et}{(1-\nu^2)}$$

P(atm)	a(μm)	t(μm)	h(μm)
40	10	0.7	2.8
100	10	0.7	2

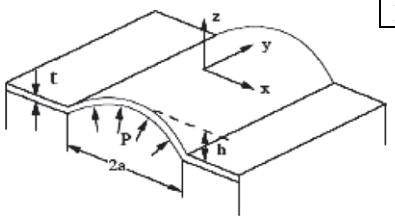

(a)

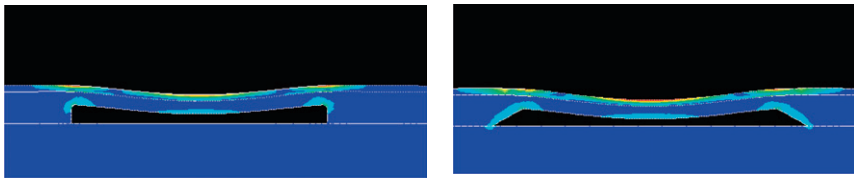

Straight sidewalls Angled (30°) sidewalls

(b)

Fig. 10. Normalized stress profiles of compressed cavities. Efficient cavity design through controlled PPC decomposition can lead to lower stress/damage during molding as shown in (b).

has a limited benefit. In order to fabricate significantly wider cavities, a new approach to creating semi-hermetic chip level packages was developed which prevents collapse of the cavity during molding. In the process described above, the PPC was slowly decomposed prior to injection molding. The overcoat was designed to withstand the molding pressure. During molding the epoxy encapsulant quickly hardens. The new approach leaves the sacrificial polymer in the cavity during the initial molding step. Once the encapsulant has hardened, the sacrificial polymer in the cavity can be decomposed creating a cavity during post mold cure of the encapsulant. Since the encapsulant is rigid during PPC decomposition, there are few size restrictions for the cavity and no metal support is necessary for the molding process.

This in situ cavity creation process needs to fit within the post mold cure temperature–time cycle. Typical post mold cure conditions are between 175 °C and 190 °C for 8 h. Thus, the sacrificial material needs to be chosen so as to completely decompose within this temperature–time profile. The sacrificial material must also be stable enough as not to decompose in the early stage of molding when the epoxy encapsulant is not rigid.

Isothermal TGA data was collected for a set of polycarbonates to identify materials that remain intact during molding and yet will decompose during post mold curing. Fig. 11 shows the weight change of PPC at 190 °C and PEC at 185 °C. Decomposition occurs slowly with complete decomposition within the target 8 h period. Little decomposition occurs within the first minutes of

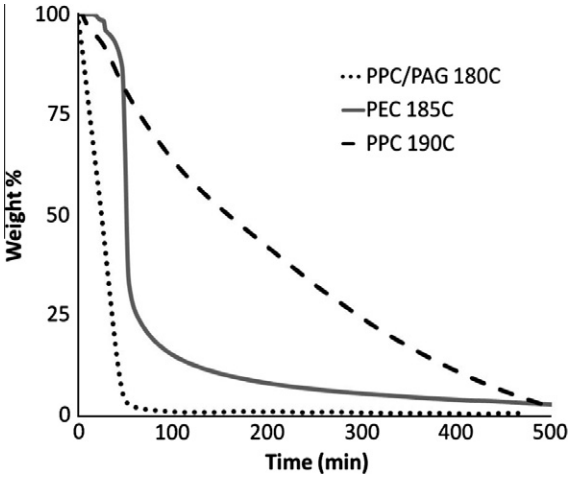

Fig. 11. Isothermal TGA of polycarbonates to be decomposed in 8 h.

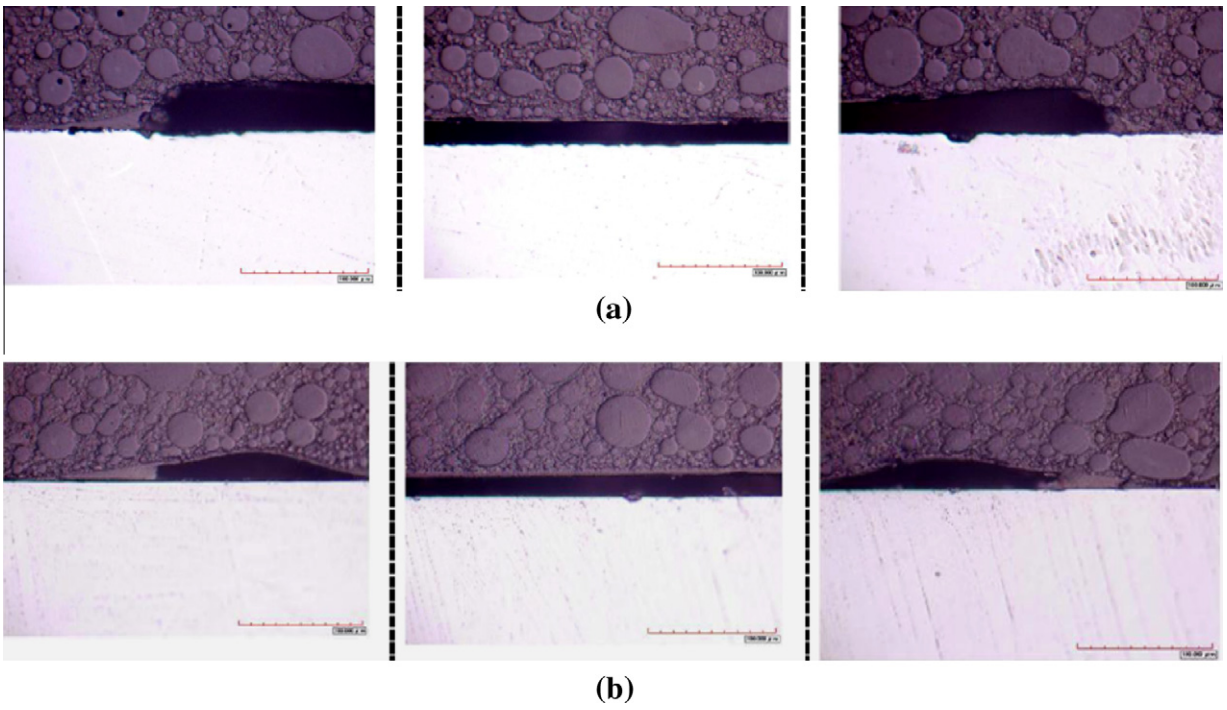

Fig. 12. Cross-sectioned in situ decomposition/cure chip level packages. (a) 2 mm diameter, 18 μm tall cavity formed by PPC decomposition at 190 °C. (b) 2 mm diameter, 12 μm tall cavity formed by PEC decomposition at 185 °C.

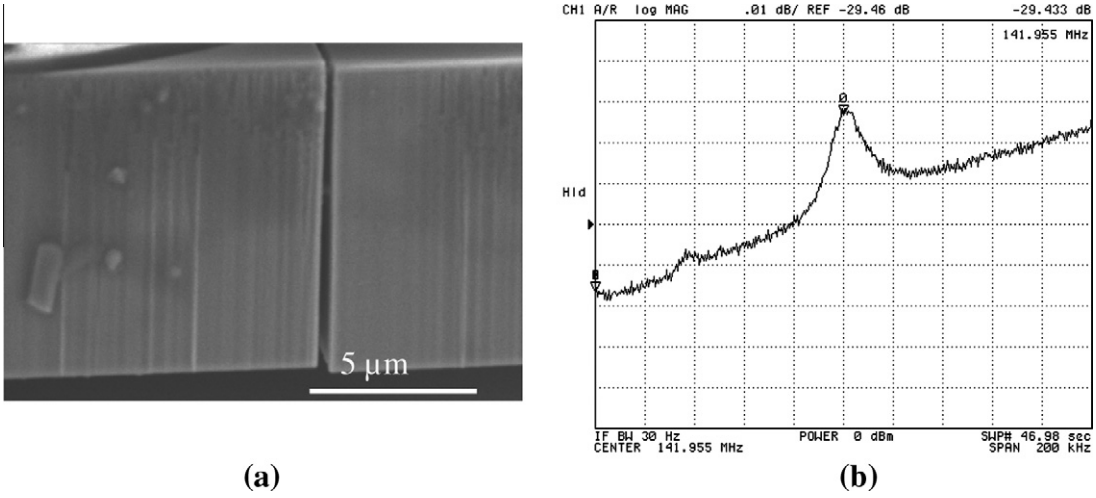

Fig. 13. A packaged capacitive resonator device. (a) Device shows clean sensing electrode. (b) Device performance was measured successfully.

the isothermal scan which corresponds to the time in the mold at high pressure. The third sacrificial polymer investigated was PPC with a 3 wt.% PAG loading. This mixture decomposes faster than the pure polymer at the target temperature and may leave a residue from the PAG loading. Each material was patterned using a POSS mask followed by RIE, as described above. The cavities were 1 and 2 mm diameter circles and squares and 10 and 18 μm tall. The patterned sacrificial material was coated with a 3 μm POSS overcoat to seal the cavities for dicing and handling. After dicing, the cavities were injection molded at 175 °C, 10 MPa for 100 s. Sets of cavities were decomposed and cured at 185 °C and 190 °C for the full 8 h. The cavities were then cross-sectioned for examination. The PPC with PAG cavities collapsed under the molding conditions, as was expected from the TGA data. This is due to the fast decomposition of the sacrificial material before the epoxy compound became rigid. The cavities formed using PPC at 185 °C had a small amount of residual PPC after 8 h decomposition, however the same cavities cured at 190 °C producing clean structures, as shown in Fig. 12(a). The PEC cavities were fully decomposed above 185 °C giving clean cavities. The PEC cavity in Fig. 12(b) was slightly deformed due to reflow of the PEC during the patterning and overcoating. Both PPC and PEC cavities exhibited no size or shape limitations. The yield on forming 1–2 mm squares and circles was high and it is expected that much larger cavities could be formed because little force is exerted on the structure when the sacrificial material decomposes.

3.5. Device packaging

High-performance, high-frequency single-crystal silicon capacitive resonators have been fabricated using the high-aspect ratio poly and single crystalline silicon (HARPSS) fabrication process

on silicon-on-insulator substrates [18]. These devices have the same cavity size as the structures shown in Fig. 2, except for the fact that the trenches were fabricated in an SOI wafer and the oxide was etched, thus releasing the cantilevers to form a functioning device with metal bond-pads. Wafer-level packaging was carried out on these devices using the POSS/PPC/Al system. After packaging, they were electrically tested for package integrity and subsequently diced for SEM analysis. Fig. 13(a) shows SEM micrographs of the device cross section. A debris-free cavity was observed. The device performance was measured, as shown in Fig. 13(b). Since the device performance could not be measured prior to packaging, it was not possible to analyze the effect of packaging on performance. However, a clean sensing electrode surface was observed after dicing which shows negligible effect of packaging on device performance. The device performance was measured and a loss of 29 dB was observed at a resonant frequency of 141 MHz, which is typical of companion devices. The losses are similar to published values on these devices [19].

The simplicity and use of existing materials gives us encouragement as to the reliability of this packaging approach. The temperature cycling and thermo-mechanical reliability of these cavities is being currently investigated. These cavities remain intact during the molding procedure under temperatures of 175 °C/8 h and 10 MPa pressure.

4. Conclusions

In this paper, we have used a novel tri-material system comprising of PPC/POSS/metal to successfully fabricate air-cavities to package MEMS devices on a wafer-level. The air-cavities are flexible in size and shape, mechanically robust, and debris-free. Nano-indentation was carried out to estimate the mechanical strength of the cavities. Compression/injection molding was carried out on cavities with different metal overcoats. Stronger and thicker metal overcoats offer better cavity-strength. 2D FEM analysis was used to correlate the experimental observations. Both FEM and analytical equations were able to predict the deformation behavior of the cavities under applied molding pressure. A novel semi-hermetic package was created using an in situ sacrificial decomposition/epoxy cure molding step for creating large cavity chip packages. Further, a set of capacitive resonator devices were successfully packaged and characterized using this process.

Acknowledgements

The authors gratefully acknowledge the intellectual and material contribution from Sumitomo Bakelite Corporation and Promerus LLC.

References

[1] N. Fritz et al., NSTI-Nanotech 2011 2 (2011) 314–317.
[2] R. Grace, M.A. Maher, Hearst Electronic Products, 2010. <http://www2.electronicproducts.com/PageSearch.aspx?FName=farc_sodtmems_nov2010.html>
[3] M. Esashi, J. Micromech. Microeng. 18 (2008) 1–13.
[4] R. Saha et al., Three dimensional air-gap structures for MEMS packaging, in: Proceedings of the 2010 Electronic Components and Technology Conference, NV, 2010, pp. 811–815.
[5] Z. Gan et al., Sensor. Actuat. A Phys. 149 (2009) 159–164.
[6] P. Joseph et al., IEEE Trans. Adv. Packag. 30 (1) (2007) 19–26.
[7] P. Monajemi et al., Characterization of a polymer based MEMS packaging technique, in: 11th International Symposium on Advanced Packaging Materials: Processes, Properties and Interface, 2006, pp. 139–144.
[8] P. Monajemi et al., A low-cost wafer level MEMS packaging technology, in: IEEE International Conference on MEMS, 2005, pp. 634–637.
[9] M. Rai-zadeh et al., A packaged micromachined switched tunable inductor, in: Proceedings of MEMS 2007, Japan, 2007, pp. 799–802.
[10] H.A. Reed et al., Compliant wafer level package (CWLP) with embedded air-gaps for sea of leads (SoL) interconnections, in: Proceedings of the IEEE2001 International Interconnect Technology Conference, pp. 151–153.
[11] S. Chen et al., J. Appl. Polym. Sci. 107 (2008) 3871–3877.
[12] L.C. Du et al., J. Appl. Polym. Sci. 92 (2004) 1840–1846.
[13] T. Spencer et al., Stabilization of the thermal decomposition of poly(propylenecarbonate) through copper ion incorporation and usein self-patterning, J. Electron. Mater. 40 (3) (2011) 1350–1363.
[14] N. Fritz et al., J. Electron. Mater. 39 (2) (2010) 149–156.
[15] X. Wu et al., J. Electrochem. Soc. 150 (9) (2003) H205–H213.
[16] <http://www.defelsko.com/technotes/adhesion_methods.htm>.
[17] J. Vlassak, W. Nix, A new bulge test technique for the determination of young modulus and Poisson ratio of thin-films, J. Mater. Res. 7 (12) (1992) 3242–3249.
[18] S. Pourkamali et al., IEEE Trans. Electron Devices 54 (8) (2007) 2017–2023.
[19] S. Pourkamali et al., IEEE Trans. Electron Devices 54 (8) (2007) 2024–2030.
[20] R. Huang et al., IEEE Trans. Device Mater. Reliab. 10 (1) (2010) 47–54.